

# A New Finite Element Model for Welding Heat Sources

JOHN GOLDAK, ADITYA CHAKRAVARTI, and MALCOLM BIBBY

A mathematical model for weld heat sources based on a Gaussian distribution of power density in space is presented. In particular a double ellipsoidal geometry is proposed so that the size and shape of the heat source can be easily changed to model both the shallow penetration arc welding processes and the deeper penetration laser and electron beam processes. In addition, it has the versatility and flexibility to handle non-axisymmetric cases such as strip electrodes or dissimilar metal joining. Previous models assumed circular or spherical symmetry. The computations are performed with ASGAR, a nonlinear transient finite element (FEM) heat flow program developed for the thermal stress analysis of welds.\* Computed temperature distributions for submerged arc welds in thick workpieces are compared to the measured values reported by Christensen<sup>1</sup> and the FEM calculated values (surface heat source model) of Krutz and Segerlind.<sup>2</sup> In addition the computed thermal history of deep penetration electron beam welds are compared to measured values reported by Chong.<sup>3</sup> The agreement between the computed and measured values is shown to be excellent.

## I. INTRODUCTION

THE problems of distortion, residual stresses, and reduced strength of a structure in and around a welded joint are a major concern of the welding industry. These problems result directly from the thermal cycle caused by the localized intense heat input of fusion welding. The high temperatures developed by the heat source cause significant metallurgical changes around the weld area of low carbon structural steels. The thermal history, particularly soaking time at high temperatures and cooling time from 800 to 500 °C, determines the microstructure and mechanical properties for a given composition. The cooling time from 400 to 150 °C is a controlling factor in the diffusion of hydrogen and the cold cracking of welds. Accurate predictions of residual stress, distortion, and strength of welded structures require an accurate analysis of the thermal cycle. The importance of a good model for the weld heat source in the analysis of the thermal cycle has been emphasized by several investigators.<sup>1,2,4-9</sup> After examining the performance of several models, a new weld heat source model is proposed that is not only more accurate than those now available but is the first one capable of handling cases that lack radial symmetry. In addition, the model smoothes the load vector which reduces the error and the computing costs of FEM analysis.

The basic theory of heat flow developed by Fourier and applied to moving heat sources by Rosenthal<sup>10</sup> in the late 1930s is still the most popular analytical method for calculating the thermal history of welds. As many researchers have shown, Rosenthal's analysis (which assumes either a point, line, or plane source of heat) is subject to serious error for temperatures in or near the fusion and heat-affected zones. In regions of the workpiece where the temperature is less than about 20 pct of the melting point, Rosenthal's solution can give quite accurate results. However, the infinite temperature at the heat source assumed in this model and the temperature sensitivity of the material thermal properties (a temperature independent mean value is assumed)

\*Developed in the Department of Mechanical and Aeronautical Engineering, Carleton University, Canada.

JOHN GOLDAK and MALCOLM BIBBY are Professors, Department of Mechanical and Aeronautical Engineering, Carleton University, Ottawa, Canada, K1S 5B6. ADITYA CHAKRAVARTI is Research Engineer, AMCA Corporation, Ottawa, Canada.

Manuscript submitted February 14, 1983.

increases the error as the heat source is approached. The effect of these assumptions and others on the accuracy of temperature distributions from the Rosenthal analysis has been discussed in detail by Myers *et al.*<sup>11</sup>

To overcome most of these limitations several authors have used FEM to analyze heat flow in welds. Since Rosenthal's point or line models assume that the flux and temperature is infinite at the source, the temperature distribution has many similarities to the stress distribution around the crack tip in linear elastic fracture mechanics. Therefore many of the FEM techniques developed for fracture mechanics can be adapted to the Rosenthal model. Certainly it would be possible to use singular FEM elements to analyze Rosenthal's formulation for arbitrary geometries. This would retain most of the limitations of Rosenthal's analysis but would permit complex geometries to be analyzed easily. However, since it would not account for the actual distribution of heat in the arc and hence would not accurately predict temperatures near the arc, this approach is not pursued here.

Pavelic *et al.*<sup>8</sup> first suggested that the heat source should be distributed. He proposed a Gaussian distribution of flux ( $W/m^2$ ) deposited on the surface of the workpiece. The subsequent works of Andersson,<sup>5</sup> Krutz and Segerlind,<sup>2</sup> and Friedman<sup>7</sup> are particularly notable. In References 2 and 7 Pavelic's disc model is combined with FEM analysis to achieve significantly better temperature distributions in the fusion and heat-affected zones than those computed with the Rosenthal model.

While Pavelic's 'disc' model is certainly a significant step forward, some authors have suggested that the heat should be distributed throughout the molten zone to reflect more accurately the digging action of the arc. This approach was followed by Paley<sup>6</sup> and Westby<sup>4</sup> who used a constant power density distribution in the fusion zone (FZ) with a finite difference analysis, but no criteria for estimating the length of the molten pool was offered. In addition, it is difficult to accommodate the complex geometry of real weld pools with the finite difference method.

A nonaxisymmetric three-dimensional heat source model is proposed in this investigation. It is argued on the basis of molten zone observations that this is a more realistic model and more flexible than any other model yet proposed for weld heat sources. Both shallow and deep penetration welds can be accommodated as well as asymmetrical situations.

The advantages of the model are demonstrated by comparing it with the Rosenthal calculations, other FEM models, and experimental results.

## II. THEORETICAL FORMULATIONS

The model proposed in this investigation is a 'double ellipsoid' configuration. It is shown that the 'disc' of Pavelic *et al.*<sup>8</sup> and the volume source of Paley and Hibbert<sup>6</sup> and Westby<sup>4</sup> are special cases of this model. In order to present and justify the double ellipsoid model, a brief description of the Pavelic 'disc' and of the Friedman<sup>7</sup> modification for FEM analysis is necessary. In addition, the mathematics of the disc is extended to spherical, ellipsoidal, and finally to the double ellipsoidal configuration. In this way both the physics and mathematics can be presented and discussed in a coherent manner.

### A. Model Considerations

The interaction of a heat source (arc, electron beam, laser) with a weld pool is a complex physical phenomenon that still cannot be modeled rigorously. At this time little is known about the distribution of pressure from the arc source, the precise effects of surface tension, buoyancy forces, and molten metal viscosity. However, it is known that these factors combine to cause weld puddle distortion and considerable stirring. Because of these complexities, modeling of the fluid flow phenomena directly is not attempted in this presentation (or elsewhere for that matter). However, because of the arc "digging" and stirring, it is clear that the heat input is effectively distributed throughout a volume in the workpiece.

The 'disc' model is more realistic than the point source because it distributes the heat input over a source area. In fact, for a preheat torch that causes no melting this may be a very accurate model indeed. However, in the absence of modeling the weld pool free boundary position, the applied tractions, and convective and radiative conditions between the weld pool and the arc, some form of idealization of the heat source is necessary to achieve a solution. The disc model does not account for the rapid transfer of heat throughout the FZ. In particular, it is not possible to predict the deep penetration FZ of an EB or laser weld with the surface disc model. A comparison of calculated thermal history data (disc model) with measured values during this investigation underscored the need for an 'effective volume source' such as the one suggested by Paley and Hibbert.<sup>6</sup> In addition, it was found necessary to generate a volume source with considerable flexibility, *i.e.*, the double ellipsoid model. With less general shapes such as a hemisphere or a single ellipsoid significant discrepancies between the computed and measured temperature distributions could not be resolved.

The size and shape of the "double ellipsoid" can be fixed, *i.e.*, the semi-axes lengths, by recognizing that the solid-liquid interface is the melting point isotherm (assuming two phase effects are negligible). At the same time weld pool temperature measurements have shown that there is little superheating in the molten zone.<sup>1</sup> The accuracy with which the heat source model predicts the size and shape of the FZ and the peak temperatures is probably the most stringent test

of the performance of the model. In this investigation it was found that the most accuracy was obtained when the ellipsoid size and shape were equal to that of the weld pool. The nondimensional system suggested by Christensen<sup>1</sup> can be used to estimate the ellipsoid parameters.

In the Paley and Hibbert<sup>6</sup> "effective volume heat source" the power density is constant throughout the molten zone. This is unrealistic physically because the stirring velocity must decay to zero at the FZ boundary and rise to a maximum at the arc-weld interface. It is undesirable mathematically because the step in the power density requires a fine mesh in a FEM analysis to obtain accurate results which is computationally unacceptable. In this investigation a Gaussian distribution is assumed centered at the origin of the heat source. Intuitively this is preferable both mathematically and physically. The results support this contention.

### B. Gaussian Surface Flux Distribution

In the 'disc' model proposed by Pavelic *et al.*,<sup>8</sup> the thermal flux has a Gaussian or normal distribution in the  $z-z$  plane (Figure 1):

$$q(r) = q(0)e^{-Cr^2} \quad [1]$$

where:

- $q(r)$  = surface flux at radius  $r$  ( $W/m^2$ )
- $q(0)$  = maximum flux at the center of the heat source ( $W/m^2$ )
- $C$  = concentration coefficient ( $m^{-2}$ ).
- $r$  = radial distance from the center of the heat source (m)

A simple physical meaning can be associated with  $C$ . If a uniform flux of magnitude  $q(0)$  is distributed in a circle of diameter  $d = 2/\sqrt{C}$ , the rate of energy input would be  $\eta IV$ , *i.e.*, the circle would receive exactly the energy from the arc. Therefore the coefficient,  $C$ , is related to the source width; a more concentrated source would have a smaller diameter  $d$  and a larger value of  $C$  (Figure 1).

Experiments have shown that a significant amount of heat is transferred by radiation and convection from the arc directly to the solid metal without passing through the molten pool. Based on this observation, Pavelic *et al.*<sup>8</sup> developed a correlation showing the amount and the distribution of this heat over the solid material. In their study,

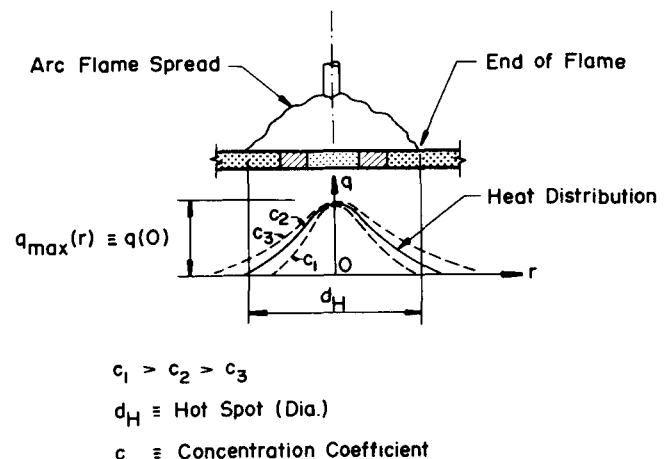


Fig. 1—Circular disc heat source (Pavelic *et al.*<sup>8</sup>).

provisions were made for convective and radiative losses from the heated plate to the surroundings as well as variable material properties.

Friedman<sup>7</sup> and Krutz and Segerlind<sup>2</sup> suggested an alternative form for the Pavelic 'disc'. Expressed in a coordinate system that moves with the heat source as shown in Fig. 2, Eq. [1] takes the form:

$$q(x, \xi) = \frac{3Q}{\pi c^2} e^{-3x^2/c^2} e^{-3\xi^2/c^2} \quad [2]$$

where:

$Q$  = energy input rate (W)

$c$  = is the characteristic radius of flux distribution (m)

It is convenient to introduce an  $(x, y, z)$  coordinate system fixed in the workpiece. In addition, a lag factor  $\tau$  is needed to define the position of the source at time  $t = 0$ . The transformation relating the fixed and moving coordinate systems is:

$$\xi = z + v(\tau - t) \quad [3]$$

where  $v$  = the welding speed (m/s). In the  $(x, y, z)$  coordinate system Eq. [2] takes the form:

$$q(x, z, t) = \frac{3Q}{\pi c^2} e^{-3x^2/c^2} e^{-3[z+v(\tau-t)]^2/c^2} \quad [4]$$

for  $x^2 + \xi^2 < c^2$ . For  $x^2 + \xi^2 > c^2$ ,  $q(x, \xi, t) = 0$ .

To avoid the cost of a full three-dimensional FEM analysis some authors assume negligible heat flow in the longitudinal direction; *i.e.*,  $\partial T/\partial z = 0$ . Hence, heat flow is restricted to an  $x$ - $y$  plane, usually positioned at  $z = 0$ . This has been shown to cause little error except for low speed high heat input welds.<sup>5</sup> The disc moves along the surface of the workpiece in the  $z$  direction and deposits heat on the reference plane as it crosses. The heat then diffuses outward ( $x$ - $y$  direction) until the weld cools.

### C. Hemispherical Power Density Distribution

For welding situations, where the effective depth of penetration is small, the surface heat source model of Pavelic, Friedman, and Krutz has been quite successful. However, for high power density sources such as the laser or electron beam, it ignores the digging action of the arc that transports heat well below the surface. In such cases a hemispherical Gaussian distribution of power density ( $\text{W}/\text{m}^3$ )

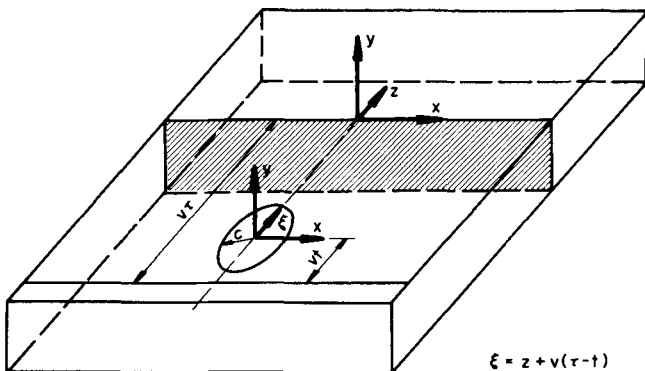


Fig. 2—Coordinate system used for the FEM analysis of the disc model according to Krutz and Segerlind.<sup>2</sup>

would be a step toward a more realistic model. The power density distribution for a hemispherical volume source can be written as:

$$q(x, y, \xi) = \frac{6\sqrt{3}Q}{c^3 \pi \sqrt{\pi}} e^{-3x^2/c^2} e^{-3y^2/c^2} e^{-3\xi^2/c^2} \quad [5]$$

where  $q(x, y, \xi)$  is the power density ( $\text{W}/\text{m}^3$ ). Eq. [5] is a special case of the more general ellipsoidal formulation developed in the next section.

Though the hemispherical heat source is expected to model an arc weld better than a disc source, it, too, has limitations. The molten pool in many welds is often far from spherical. Also, a hemispherical source is not appropriate for welds that are not spherically symmetric such as strip electrode, deep penetration electron beam, or laser beam welds. In order to remove these constraints, and make the formulation more accurate, an ellipsoidal volume source is now proposed.

### D. Ellipsoidal Power Density Distribution

The Gaussian distribution of the power density in an ellipsoid with center at  $(0, 0, 0)$  and semi-axes  $a, b, c$  parallel to coordinate axes  $x, y, \xi$  can be written as:

$$q(x, y, \xi) = q(0) e^{-Ax^2} e^{-By^2} e^{-C\xi^2} \quad [6]$$

where  $q(0)$  is the maximum value of the power density at the center of the ellipsoid.

Conservation of energy requires that:

$$2Q = 2\eta VI = 8 \int_0^x \int_0^y \int_0^\xi q(0) e^{-Ax^2} e^{-By^2} e^{-C\xi^2} dx dy d\xi \quad [7]$$

where:

$\eta$  = heat source efficiency

$V$  = voltage

$I$  = current

Evaluating Eq. [7] produces the following:

$$2Q = \frac{q(0)\pi\sqrt{\pi}}{\sqrt{ABC}} \quad [8]$$

$$q(0) = \frac{2Q\sqrt{ABC}}{\pi\sqrt{\pi}} \quad [9]$$

To evaluate the constants,  $A, B, C$ , the semi-axes of the ellipsoid  $a, b, c$  in the directions  $x, y, \xi$  are defined such that the power density falls to  $0.05q(0)$  at the surface of the ellipsoid. In the  $x$  direction:

$$q(a, 0, 0) = q(0) e^{-Aa^2} = 0.05q(0) \quad [10]$$

Hence

$$A = \frac{\ln 20}{a^2} \approx \frac{3}{a^2} \quad [11]$$

Similarly

$$B \approx \frac{3}{b^2} \quad [12]$$

$$C \approx \frac{3}{c^2} \quad [13]$$

Substituting  $A, B, C$  from Eqs. [11] to [13] and  $q(0)$  from

Eq. [9] into Eq. [6]:

$$q(x, y, \xi) = \frac{6\sqrt{3}Q}{abc\pi\sqrt{\pi}} e^{-3x^2/a^2} e^{-3y^2/b^2} e^{-3\xi^2/c^2} \quad [14]$$

The coordinate transformation (Eq. [3], Figure 2) can be substituted into Eq. [14] to provide an expression for the ellipsoid in the fixed coordinate system.

$$q(x, y, z, t) = \frac{6\sqrt{3}Q}{abc\pi\sqrt{\pi}} e^{-3x^2/a^2} e^{-3y^2/b^2} e^{-3[z+v(\tau-t)]^2/c^2} \quad [15]$$

If heat flow in the  $z$  direction is neglected, an analysis can be performed on the  $z$ - $y$  plane located at  $z = 0$  which is similar to the 'disc' source (Figure 2). Where the ellipsoidal source intersects this plane the power density is calculated for each time increment.

#### E. Double Ellipsoidal Power Density Distribution

Calculation experience with the ellipsoidal heat source model revealed that the temperature gradient in front of the heat source was not as steep as expected and the gentler gradient at the trailing edge of the molten pool was steeper than experimental experience. To overcome this limitation, two ellipsoidal sources are combined as shown in Figure 3. The front half of the source is the quadrant of one ellipsoidal source, and the rear half is the quadrant of another ellipsoid. The power density distribution along the  $\xi$  axis is shown in Figure 3. In this model, the fractions  $f_f$  and  $f_r$  of the heat deposited in the front and rear quadrants are needed, where  $f_f + f_r = 2$ . The power density distribution inside the front quadrant becomes:

$$q(x, y, z, t) = \frac{6\sqrt{3}f_f Q}{abc\pi\sqrt{\pi}} e^{-3x^2/a^2} e^{-3y^2/b^2} e^{-3[z+v(\tau-t)]^2/c^2} \quad [16]$$

Similarly, for the rear quadrant of the source the power density distribution inside the ellipsoid becomes:

$$q(x, y, z, t) = \frac{6\sqrt{3}f_r Q}{abc\pi\sqrt{\pi}} e^{-3x^2/a^2} e^{-3y^2/b^2} e^{-3[x+v(\tau-t)]^2/c^2} \quad [17]$$

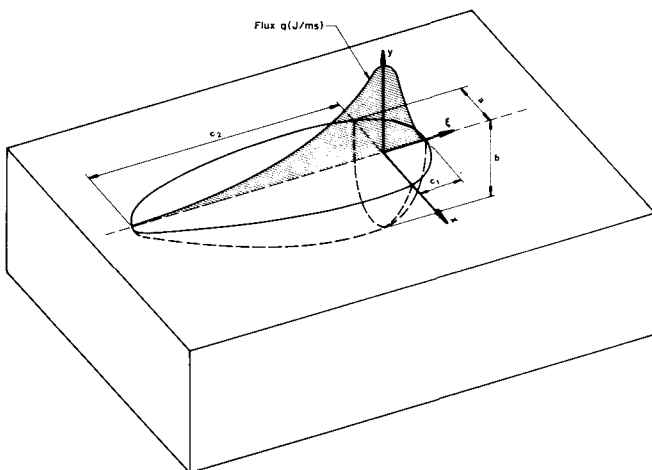


Fig. 3—Double ellipsoid heat source configuration together with the power distribution function along the  $\xi$  axis.

In Eqs. [16] and [17], the parameters  $a, b, c$  can have different values in the front and rear quadrants since they are independent. Indeed, in welding dissimilar metals, it may be necessary to use four octants, each with independent values of  $a, b$ , and  $c$ .

## FEM CALCULATIONS

### III. EVALUATION OF THE DOUBLE ELLIPSOID MODEL

In order to minimize the computing cost the initial analysis was done in the plane normal to the welding direction as shown in Figures 4 and 5. Thus, heat flow in the welding direction was neglected. The above simplification is accurate in situations where comparatively little heat flows from the arc in the welding direction. This is reasonable when the arc speed is high. An estimate of the effect of this approximation has been given by Andersson<sup>5</sup> who argues that the errors introduced by neglecting heat flow in the direction of the moving electrode are not large, except in the immediate vicinity of the electrode.

#### A. Verification of the Model

In order to demonstrate the flexibility and assess the validity of the double ellipsoidal heat source model two quite different welding situations were considered. The first case analyzed was a thick section (10 cm (4 inches)) submerged arc bead on plate (low carbon structural steel – 0.23 pct C) weld shown schematically in Figure 4. The welding conditions are contained in the figure. Christensen<sup>1,4</sup> reported a

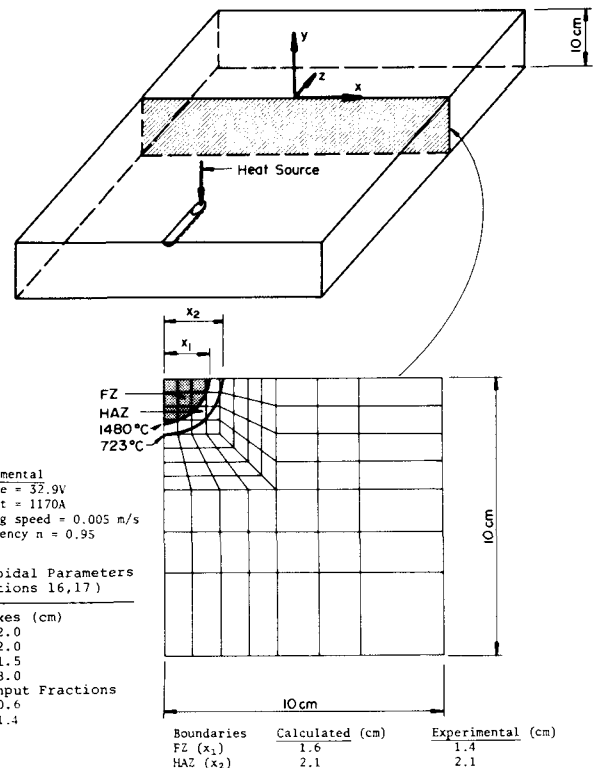


Fig. 4—Experimental arrangement and FEM mesh for the thick section bead on plate weld reported by Christensen.<sup>1</sup>

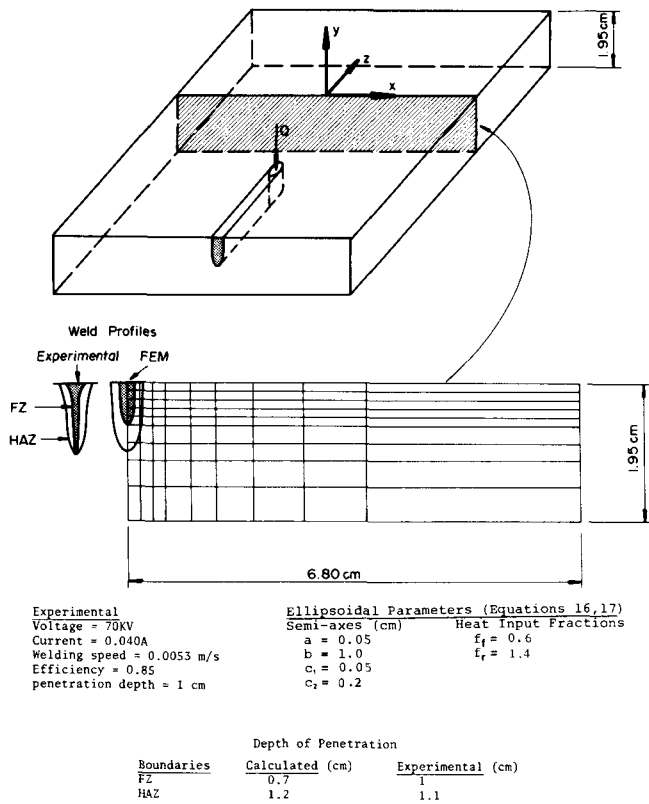


Fig. 5—Experimental arrangement and FEM mesh for the deep penetration weld reported by Chong.<sup>3</sup>

cooling time 800 to 500 °C of 37 seconds for this weld and the FZ and HAZ sizes shown in the diagram. Shown also in the figure is the FEM mesh used to calculate these quantities. It is two-dimensional in  $x$  and  $y$  as previously explained. The temperature distribution in the 'cross-section analyzed' is calculated for a series of time steps as the heat source passes. In this way the FZ and HAZ cross-sectional sizes can be determined, and from the time step-temperature data the cooling time 800 to 500 °C is calculated.

The second welding situation is taken from the work of Chong.<sup>3</sup> It is a partial penetration electron beam bead on plate (low carbon steel—0.21 pct C) weld. Traditionally the Rosenthal 2D model would be used to analyze this weld. However, there is some heat flow in the through thickness dimension since the penetration is partial and, of course, the idealized line heat source is suspect. The ellipsoidal model can be easily adapted to this weld geometry by selecting appropriate characteristic ellipsoidal parameters (see Section III-B below). A cooling time (800 to 500) of 1.9 seconds was measured by Chong<sup>3</sup> and the FZ and HAZ dimensions were reported.

The temperature dependent volumetric specific heat and thermal conductivity published by BISRA<sup>16</sup> and replotted in Figures 6 and 7 were used for all calculations. In the liquid range (1480 °C) a thermal conductivity of 120 W/m<sup>2</sup> C was assumed, in order to simulate to a first approximation the heat transfer by convective stirring in the molten pool. A heat of fusion of  $2.1 \times 10^9$  J/m<sup>3</sup> and a heat of transformation of  $5.5 \times 10^7$  J/m<sup>3</sup> were associated with the melting

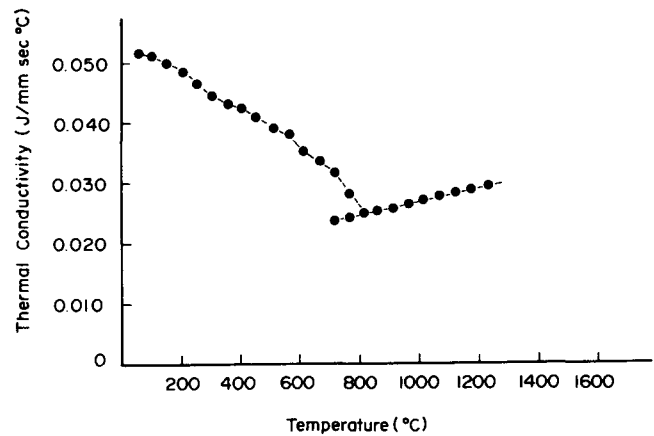


Fig. 6—Temperature dependence of the thermal conductivity for low carbon steels.<sup>16</sup>

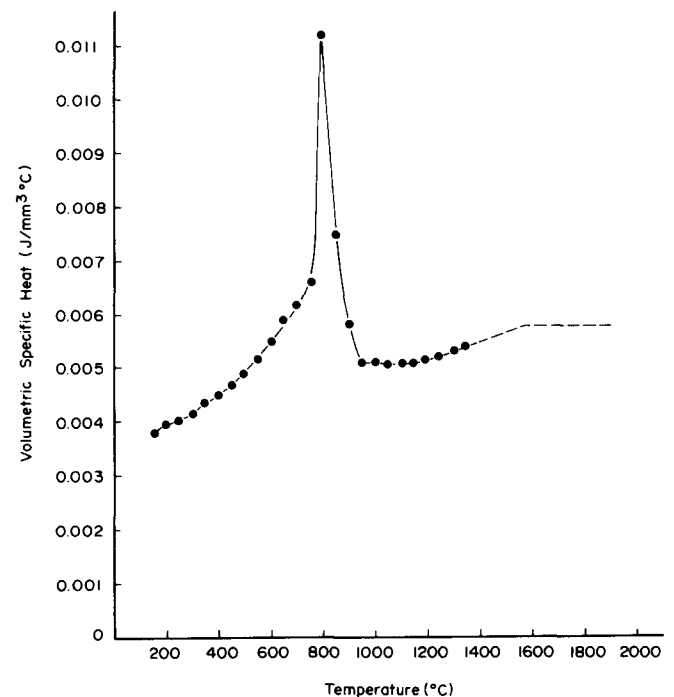


Fig. 7—Temperature dependence of the volumetric heat capacity for low carbon steels.<sup>16</sup>

(fusion) and transformation temperatures, respectively. This is done by computing the specific heat from the change in enthalpy at each time step. An algorithm to solve the Stefan problem for moving phase boundaries is being implemented.

For the radiative and convective boundary conditions, a combined heat transfer coefficient was calculated from the relationship.<sup>14</sup>

$$H = 24.1 \times 10^{-4} \epsilon T^{1.61} \quad [18]$$

where  $\epsilon$  is the emissivity or degree of blackness of the surface of the body. A value of 0.9 was assumed for  $\epsilon$ , as recommended for hot rolled steel.<sup>14</sup>

### B. Estimates of Characteristic Flux Distribution Parameters

As shown in Figure 3 there are four characteristic length parameters that must be determined. Physically these parameters are the radial dimensions of the molten zone in

front, behind, to the side, and underneath the arc. If the cross-section of the molten zone is known from experiment, these data may be used to fix the heat source dimensions. For example, the width and depth are taken directly from a cross-section of the weld. In the absence of better data, the experience of these authors suggests it is reasonable to take the distance in front of the heat source equal to one-half the weld width and the distance behind the heat source equal to twice the width. If cross-sectional dimensions are not available Christensen's expressions<sup>1</sup> can be used to estimate these parameters. Basically Christensen defines a nondimensional operating parameter and nondimensional coordinate systems. Using these expressions, the weld pool dimensions can be estimated.

The nondimensional Christensen method was used to fix the ellipsoidal flux distribution parameters for the thick section bead on plate weld shown in Figure 4. The cross-sectional dimensions were reported by Chong, and the half-width dimension was applied to the flux distance in front of the EB heat source while the twice-width distance was applied behind the electron beam. The heat input fractions used in the computations were based on a parametric study of the model. Values of  $f_f = 0.6$  and  $f_r = 1.4$  were found to provide the best correspondence between the measured and calculated thermal history results.

#### IV. RESULTS

##### A. Analysis of the Thick Plate Problem

For the solution of this problem, only one-half of the cross section is considered, because of symmetry. All the boundaries except the top surface were assumed insulated. On the top surface, the portion just under the arc was assumed insulated during the time the arc was playing upon the surface. A combined convection and radiation boundary condition (Eq. [18]) was assumed on the remainder of the top surface. The domain was discretized into 81 eight node quadrilateral isoparametric elements to form the finite element mesh (Figure 4).

The temperature distribution along the width perpendicular to the weld center line at 11.5 seconds after the arc passed is shown in Figure 8. It is compared to the experimental data from Christensen *et al.*<sup>1</sup> and the finite element analysis of the same problem by Krutz and Segerlind<sup>2</sup> where a disc-shaped heat source (Eq. [4]) was used. As expected, the ellipsoidal model gives better agreement with experiment than the disc.

The fusion and heat-affected zone boundary positions predicted by these FEM calculations are in good agreement with the experimental data, as shown in Figure 4. In addition, the FEM cooling times (800 to 500 °C) are much closer to the experimental value (within 5 pct—Table I) than the cooling time calculated by the Rosenthal's analysis (41 pct). The FEM cooling time (39 seconds) is slightly larger than the experimental value (37 seconds). This may be due to neglecting the longitudinal heat flow. The radiation-convection applied to the top surface had little effect on the thermal cycle or the FZ-HAZ boundaries. This is to be expected for thick section welds where the heat flow is dominated by conduction.

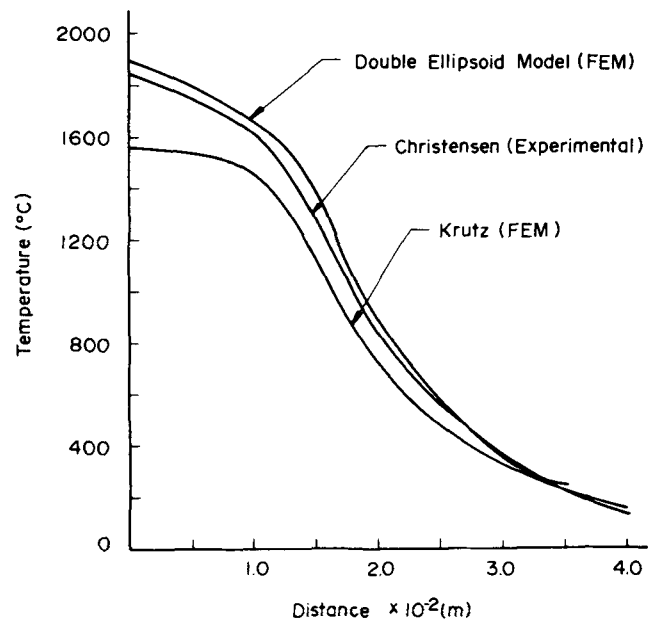


Fig. 8—Temperature distribution along the top of the workpiece perpendicular to the weld 11.5 s after the heat source ( $\xi = 0$ ) has passed the reference plane (x direction—Figs. 2 and 4). Experimental results of Christensen<sup>1</sup> compared to FEM computed values of Krutz and Segerlind<sup>2</sup> (disc model) and the FEM computed values using the double ellipsoid model. Experimental conditions documented in Fig. 4.

**Table I. A Comparison of the Computed and Experimental Cooling Time (800 to 500 °C) for the Thick Section Bead-On-Plate Weld**

Calculation Method	Cooling Time (Seconds)	Difference <sup>4</sup> (Percentage)
Experimental <sup>1</sup>	37	—
Analytical <sup>2</sup>	22	-41
FEM (Double Ellipsoid) <sup>3</sup>	39	+ 5

(1) Experimental: submerged arc—32.9 V, 1170 A, 0.005 mls; workpiece—0.23 pct carbon steel plate, 100 mm thick (Christensen *et al.*)<sup>1</sup>  
(2) Conventional Rosenthal analytical solution,<sup>10</sup> mean thermal conductivity  $k = 41$  W/(m °C) and efficiency = 0.95  
(3) Finite element double ellipsoid heat source geometry: size and shape fixed by the Christensen method,<sup>1</sup> variable thermal properties  
(4) Difference is calculated value minus experimental value.

##### B. Analysis of the Electron Beam Weld

Rosenthal's analytic solution for a line source is often applied to electron beam and laser welds where there is significant penetration into the workpiece. In so doing the heat flow is assumed to be entirely two-dimensional. If the penetration is almost entirely through the workpiece this can be justified (although the line source is still suspect as discussed previously). However, the line source is often applied to deep welds with partial penetration even though there must be heat flow in the through thickness direction and the heat flow is not truly two-dimensional. The partial penetration electron beam weld reported by Chong<sup>3</sup> is such a case. The penetration is 1 cm in a 1.95 cm thick plate.

The FEM mesh used to analyze this weld is shown in Figure 5. Once again 81 eight node quadratic elements were used. Smaller elements were specified where the steepest

temperature gradients were expected. The convection-radiation boundary condition was applied to the top surface. As in the previous case, no effect from convective cooling was observed because the heat flow is conduction dominated.

The FZ boundary depth (0.7 cm) predicted by FEM is somewhat less than the experimental value of 1.0 cm (Figure 5). In addition, the FEM FZ/HAZ contour is not nearly as sharp at the bottom as the real weld. These effects are thought to be caused by neglecting the longitudinal heat flow which reduces the gradient and spreads the contours in the plane normal to the welding direction. A full three-dimensional analysis is underway to clarify this point.

As shown in Table II, the cooling time (800 to 500 °C) calculated with the FEM double ellipsoid model is within 5 pct of the measured value. On the other hand, Rosenthal's line source analysis is in error by 21 pct from the experimental values. At the same time, Rosenthal's point source also differs by a similar amount. It is evident that the values calculated with the FEM model are considerably better than those determined by conventional analysis.

## V. CONCLUSIONS

1. A double ellipsoid model has been presented for a welding heat source that has the capability of analyzing the thermal history of shallow and deep penetration welds or asymmetrical welds such as strip electrodes.
2. A comparison of the temperature distribution around a weld demonstrates that the double ellipsoid model which spreads the thermal load throughout the weld pool is more accurate than the disc model where the thermal load is applied only to the surface of the weld.
3. The FEM double ellipsoid cooling time values (800 to 500 °C) for both shallow and deep penetration welds are much closer to the experimental values than those calcu-

lated from Rosenthal's analysis. The fact that the FEM values are always slightly higher than the experimental values may be due to neglecting the longitudinal flow heat flow.

4. For the deep penetration and heavy plate welds considered in this investigation, radiation-convection losses from the workpiece near the heat source were found to be negligible.
5. The double ellipsoid model applied to a deep penetration weld does not predict the sharp point at the bottom of the FZ and HAZ observed in experiments. This is thought to be due to neglecting the heat flow in the longitudinal direction which reduces the gradient and separates the temperature contours in the plane normal to the welding direction.

## ACKNOWLEDGMENTS

The financial support of the National Science and Engineering Research Council NRCA2992 (J. Goldak) and NRCA4601 (M. Bibby), Department of Energy, Mines and Resources (J. Goldak), and of the AMCA Corp. (Ottawa) are gratefully acknowledged.

## REFERENCES

1. N. Christensen, L. de V. Davies, and K. Gjermundsen: *British Welding Journal*, 1965, vol. 12, pp. 54-75.
2. G. W. Krutz and L. J. Segerlind: *Welding Journal Research Supplement*, 1978, vol. 57, pp. 211s-16s.
3. L. M. Chong: *Predicting Weld Hardness*, M. Eng. Thesis, Department of Mechanical and Aeronautical Engineering, Carleton University, Ottawa, Canada, 1982, pp. 56-57.
4. O. Westby: *Temperature Distribution in the Workpiece by Welding*, Department of Metallurgy and Metals Working, The Technical University, Trondheim, Norway, 1968.
5. B. A. B. Andersson: *Journal of Engineering Materials and Technology*, Trans. ASME, 1978, vol. 100, pp. 356-62.
6. Z. Paley and P. D. Hibbert: *Welding Journal Research Supplement*, 1975, vol. 54, pp. 385s-92s.
7. E. Friedman: *Journal Pressure Vessel Technology*, Trans. ASME, 1975, vol. 97, pp. 206-13.
8. V. Pavelic, R. Tanbakuchi, O. A. Uyehara, and P. S. Myers: *Welding Journal Research Supplement*, 1969, vol. 48, pp. 295s-305s.
9. K. Masubuchi: *Control of Distortion and Shrinkage in Welding*, Welding Research Council Bulletin, New York, NY, 1970, no. 169.
10. D. Rosenthal: *Trans. ASME*, 1946, vol. 68, pp. 849-65.
11. P. S. Myers, O. A. Uyehara, and G. L. Borman: *Fundamentals of Heat Flow in Welding*, Welding Research Council Bulletin, New York, NY, 1967, no. 123.
12. E. Friedman: *Welding Journal Research Supplement*, 1978, vol. 57, pp. 161s-66s.
13. W. F. Hess, L. L. Merrill, E. F. Nippes Jr., and A. P. Bunk: *Welding Journal Research Supplement*, 1943, vol. 23, pp. 377s-422s.
14. R. R. Rykalin: *Energy Sources for Welding*, Houdrement Lecture, International Institute of Welding, London, 1974, pp. 1-23.
15. V. A. Vinokurov: *Welding Stresses and Distortions*, The British Library, Lending Division, Translated from Russian into English by J. E. Baker, 1977, pp. 118-19.
16. The British Iron and Steel Research Association, *Physical Constants of Some Commercial Steels at Elevated Temperatures*, London Butterworths Scientific Publications, 1953.

**Table II. A Comparison of the Computed and Experimental Cooling Time (800 to 500 °C) for a Deep (Partial) Penetration Electron Beam Weld**

Calculation Method	Cooling Time (Seconds)	Difference <sup>4</sup> (Percentage)
Experimental <sup>1</sup>	1.9	—
Analytical (2D) <sup>2</sup>	2.4	+21
Analytical (3D) <sup>2</sup>	1.4	-21
FEM (Double Ellipsoid) <sup>3</sup>	2.0	+ 5

(1) Experimental: electron beam weld—70,000 V, 0.04 A, 0.0053 m/s, 0.01 m penetration; workpiece—0.24 pct carbon steel, 19 mm thick (Chong)<sup>3</sup>

(2) Conventional Rosenthal analytical solutions,<sup>10</sup> mean thermal conductivity = 41 W/(m °C), mean volumetric specific heat capacity =  $4.5 \times 10^6$  J/(m<sup>3</sup> °C), heat source efficiency = 0.85

(3) Finite element double ellipsoid model: cross-sectional size taken from measurements of Chong,<sup>3</sup> variable thermal properties

(4) Difference is calculated value minus experimental value.